Impact of strain and surface reconstruction on long-range diffusion of Ge atoms on Ge(111) surface

R. A. Zhachuk [1,*] A. V. Latyshev [1] and J. Coutinho [2]

[1]*Institute of Semiconductor Physics, Prospekt Lavrentyeva 13, Novosibirsk 630090, Russia*

[2]*I3N, Department of Physics, University of Aveiro, Campus Santiago, 3810-193 Aveiro, Portugal*

(Received 21 April 2023; revised 2 June 2023; accepted 16 June 2023; published 26 June 2023)

We investigate the effect of surface reconstruction and strain on diffusion of adsorbed Ge atoms on Ge(111)-5 × 5 and Ge(111)-7 × 7 surfaces by means of first-principles calculations. Stable adsorption sites and their energies, diffusion paths, and corresponding activation barriers are reported. We demonstrate that the decisive migration path is located near the corner holes of surface structures, and they are associated with formation of weak bonds between the adsorbed Ge atom and surface dimers (within the 5 × 5 or 7 × 7 structures). The results show that Ge diffusion rates on 5 × 5 and 7 × 7 reconstructed Ge(111) surfaces should be similar. Conversely, the diffusion barrier on a compressively strained Ge(111) surface is considerably higher than that on a strain-free surface, thus explaining previous experimental results. Comparable diffusion rates on 5 × 5 and 7 × 7 reconstructed surfaces are explained by the identical local atomic arrangements of these structures. The increase of the migration barrier on a strained surface is explained by dimer bond strengthening upon surface compression, along with a weakening of bonds between the adsorbed Ge and dimer atoms.

DOI: 10.1103/PhysRevB.107.245305

I. INTRODUCTION

Surface diffusion is an important topic with direct impact on thin-film growth and its morphology and nanostructure formation. Besides temperature, several parameters can be used to change the surface diffusivity. For example, it can be influenced by the surface atomic structure, substrate chemical composition, type of diffusing species, or surface strain.

The strain dependence of atomic diffusion on metal surfaces, where bonds are omnidirectional, is relatively well understood. Surface compressive strain pushes the diffusing atoms away from the crystal surface so that they experience a less corrugated surface potential. As a result, the energy barrier for the metallic systems is found to decrease with increasing compressive strain [1,2].

On the other hand, strain and structure dependence of diffusion on semiconductor surfaces can be more complex because of the directional and localized nature of bonds between surface and adsorbed atoms. For instance, strong diffusion anisotropy has been observed on the Si(001)-2 × 1 surface: The diffusivity parallel to dimer rows is faster than that perpendicular to the rows by three orders of magnitude [3–5]. With increasing tensile strain, the diffusivity across the dimer rows is further frustrated (according to both experiments and first-principles calculations [6,7]) while that along the dimer rows is enhanced (according to calculations of Shu *et al.* [6]) or does not change (according to experiments of Zoethout and co-workers [7]).

Experimental studies of surface diffusion on Si(111)-7 × 7 also revealed an interesting phenomenon: The mobility of adsorbed atoms inside the Si(111)-7 × 7 half unit cells (HUCs) was in many cases found to be high at room temperature, while under the same conditions, hops between neighboring HUCs were rare [8–17]. This is somewhat unexpected since Si(111)-7 × 7 HUCs contain a high density of dangling bonds, to which adsorbed atoms can connect strongly. The above findings were partially explained by a first-principles study showing that the high radical density on Si(111)-7 × 7 HUCs is precisely at the origin of the low migration barriers. Accordingly, concurrent breaking and formation of closely spaced bonds within the HUCs lead to a relatively flat potential energy surface for adatom motion [18,19].

Cherepanov and Voigtländer studied the surface diffusion of adatoms (Ge or Si) on Ge(111) and Si(111) surfaces in the range $T = 400$–700 K by following the density of two-dimensional islands formed upon submonolayer deposition by scanning tunneling microscopy (STM) [20,21]. By preparing substrates that differed by a single parameter only, they were able to experimentally separate the influence of various factors impacting the density of formed islands. The change of the surface diffusion barrier was estimated from the change of island density with the help of the Venables theory of nucleation [22], i.e., assuming typical values for the critical nucleation size and preexponential factors. It was found that the most influential factors were the substrate and deposited materials (Si or Ge). A relatively slower diffusivity of Si (in comparison to that of Ge) was found on both Si(111) and Ge(111) substrates, and that was attributed the formation of stronger Si-X bonds (as compared to Ge-X ones), with $X = \{\text{Si, Ge}\}$. It was also shown that the change of Ge(111) surface structure from 7 × 7 to 5 × 5 had a negligible effect on the island formation rate (surface diffusivity), and more surprisingly, the diffusion barrier for Ge (Si) adatoms increased with increasing surface compressive strain. The latter observations are difficult to understand and were left unexplained [20,21].

*zhachuk@gmail.com

 ©2023 American Physical Society

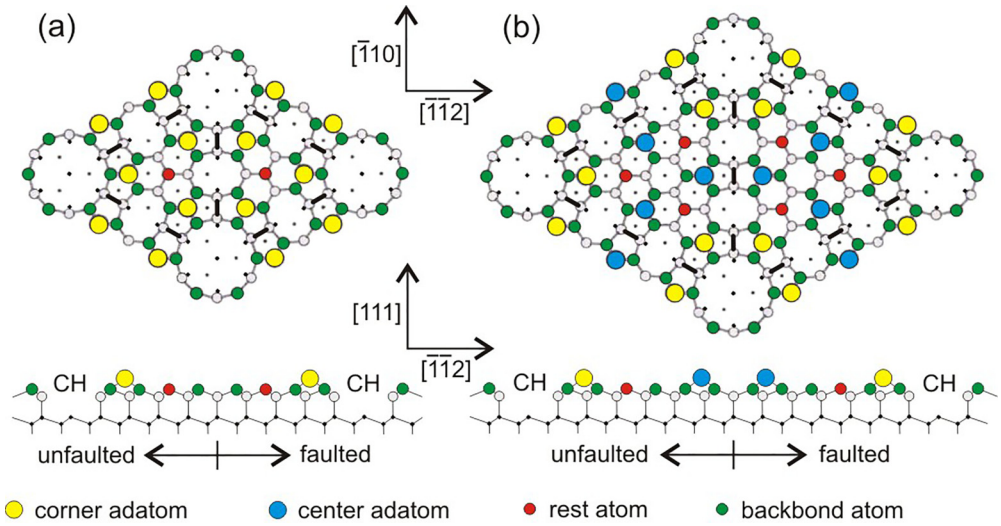

FIG. 1. Top (upper panels) and sectional (lower panels) views of (a) 5×5 and (b) 7×7 structures of Ge(111) surface according to the DAS model [23]. Sectional views are in the $(1\bar{1}0)$ plane cutting the long diagonal of the 5×5 and 7×7 surface unit cells, showing the nearest neighbor bonding structure. Thick rods (in the top views) edging the perimeter of the cells represent Ge-Ge dimers. CH stands for corner hole.

The present work aims at addressing the above questions by means of atomistic first-principles calculations. We find that the migration path on both 5×5 and 7×7 reconstructed surfaces is located near the corner holes of the surface structure, and they involve the formation of weak bonds between adsorbed Ge atoms and surface dimers. It is shown that equal diffusion rates on 5×5 and 7×7 reconstructed surfaces are due to the identical local atomic arrangements of these structures. On the other hand, the diffusion barrier increase under surface compression is due to strengthening of surface dimer bonds, accompanied by weakening of bonds between adsorbed Ge and dimer atoms at the transition state.

II. CALCULATION DETAILS

The calculations were carried out using the pseudopotential [24] density functional theory (DFT) SIESTA code [25,26] within the generalized gradient approximation (GGA) to the exchange and correlation interactions between electrons as parametrized by Perdew, Burke, and Ernzerhof (PBE) [27]. The Kohn-Sham wave functions were described with help of linear combinations of atom-centered orbitals of the Sankey-Niklewski type, which included multiple zeta orbitals and polarization functions [25].

The supercell geometries consisted of repeating slabs of four (111)-oriented Ge bilayers separated by a 16 Å wide vacuum gap along the Cartesian z direction. All Ge dangling bonds at the unreconstructed bottom surface were saturated by hydrogen atoms, and those Ge-H units were kept frozen during atomic relaxations. Top layers of the slabs were modified according to the dimer-adatom-stacking fault (DAS) atomic models of 5×5 and 7×7 reconstructions [23], as depicted in Fig. 1. According to that model, each 5×5 (7×7) unit cell contains (i) a stacking fault in one of its HUCs between the first and second bilayer, (ii) a corner hole (CH) corresponding to one missing atom in second atomic layer (first bilayer) and, hence, leaving a dangling bond at its center atom in the third atomic layer (second bilayer), (iii) 6 (9) dimers forming domain walls along the boundary of one of its HUCs, (iv) 6 (12) adatoms in T_4 sites in a 2×2-like environment, and (v) 2 (6) rest atoms in the first atomic layer, the dangling bonds of which are not saturated by bonding to the adatoms. The two nonequivalent HUCs with and without stacking faults are called faulted and unfaulted, respectively.

Atoms from the two upper Ge layers of the slab and the adsorbed Ge atom contributed with two sets of s and p orbitals plus one d orbital to describe the Kohn-Sham states. On the other hand, Ge atoms from the two bottommost layers of the slab had only one set of s and p orbitals, and all H atoms were assigned a single s orbital. The electron density and potential terms were calculated on a real-space grid with spacing equivalent to a plane-wave cutoff of 200 Ry. For the Brillouin-zone (BZ) integration of the 5×5 surface structure we used a $4 \times 4 \times 1$ **k**-point grid [28], while for the 7×7 structure we used Γ-point only.

The energetics of a Ge adatom on the Ge(111) surface was studied by means of mapping the potential energy surfaces (PESs) as a function of the adatom position. PES maps were produced for positions of the adsorbed Ge probe atom within the symmetry-irreducible wedge of each cell [18]. PES data for the whole cells were unfolded by applying all C_{3V} symmetry operations to the irreducible PES wedge data. For each xy coordinate, the adsorbed atom was initially placed approximately 3 Å above the surface, and its z coordinate was allowed to relax while the coordinates in the xy plane were kept fixed. The positions of all remaining atoms, but the bottom Ge-H units, were fully optimized until atomic forces became less than 0.01 eV/Å. For a 5×5 (7×7) supercell, a total of 66 (120) points, forming the irreducible hexagonal grid with 1.2 Å spacing, were initially calculated. This method has been successfully used by several authors (see for instance Refs. [18,29–31] for a few works in silicon).

After identification of the main energy minima, additional points were calculated along the energy paths connecting them, resulting in a spacing of 0.6 Å. The exact energies of local energy minima on PES were calculated with a

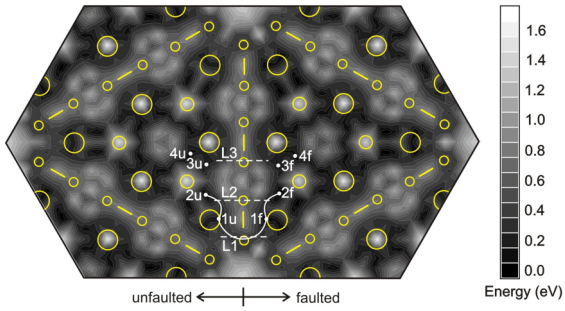

FIG. 2. PES for an adsorbed Ge atom on unstrained Ge(111)-7 × 7 surface. Dark (bright) regions indicate energy minima (maxima) and, hence, favorable adsorption positions (unstable/transition-state regions). The contour spacing is 0.1 eV. Large circles point to adatom locations, medium circles to rest atoms, small circles connected by rods indicate dimers along the HUC perimeter. White dots with labels 1u-4u and 1f-4f mark the deepest PES minima inside of unfaulted (u) and faulted (f) HUCs, respectively. Dashed lines across the HUC border (with labels L1–L3) mark the positions of calculated migration paths. The solid line connecting the deepest energy minima in faulted and unfaulted HUCs (2u and 2f) is the minimum energy path for border crossing.

free-moving probe atom placed near the local energy minima. Judging from the calculated data, the numerical uncertainty of calculated energy barriers is estimated at about 0.1 eV.

III. RESULTS AND DISCUSSION

Let us first discuss the Ge/Ge(111)-7 × 7 system. Figure 2 shows the calculated PES for the adsorption of a Ge atom on the unstrained Ge(111)-7 × 7 surface. Dark (bright) regions indicate energy minima (maxima). Relative energies of PES minima on Ge(111)-5 × 5 and Ge(111)-7 × 7 surfaces are given in Table I. From the PES, one can see that the Ge(111)-7 × 7 PES is very corrugated. The deepest PES minima are located inside of the unfaulted (1u–4u) and faulted (1f–4f) HUCs next to adatoms and rest atoms, where the adsorbed atom can saturate several surface dangling bonds. From visual inspection of the relaxed coordinates we conclude that all these PES minima are associated with the formation

TABLE I. Relative energies (eV) of local stable adsorption sites for a Ge atom on unstrained Ge(111)-7 × 7, Ge(111)-5 × 5 surfaces and Ge(111)-5 × 5 surface compressively strained by 4%. *N* is the site number according to Figs. 2 and 5. For each studied surface, the energy of the most stable site is considered the origin of the energy scale.

	Surface structure					
	7 × 7 unstrained		5 × 5 unstrained		5 × 5 strained	
N	u	f	u	f	u	f
1	0.22	0.11	0.20	0.09		0.19
2	0.07	0.00	0.07	0.00	0.18	
3	0.15	0.12				
4	0.09	0.11				
5					0.28	0.00

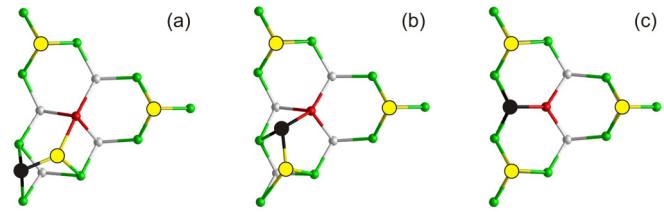

FIG. 3. Atomic structures pertaining to the PES minima of Ge atom on the Ge(111)-5 × 5 HUC (top view). The coloring scheme is identical to that of Fig. 1, with the black ball representing the adsorbed Ge atom. (a) Unstrained 5 × 5, PES minima 1u (1f). Same local atomic arrangement is observed for unstrained 7 × 7, 1u (1f) and strained 5 × 5, 1f. (b) Unstrained 5 × 5, PES minima 2u (2f). Same local atomic arrangement is observed for unstrained 7 × 7, 2u (2f), 3u (3f), 4u (4f) and strained 5 × 5, 2u. (c) Strained 5 × 5, PES minima 5u (5f) represented in Fig. 5.

of dimers consisting of an adsorbed (diffusing) Ge atom and 7 × 7 adatom. Atomic structures relevant to the PES minima on Ge(111)-5 × 5 and Ge(111)-7 × 7 surfaces are shown in Fig. 3.

Essentially, Figs. 3(a) and 3(b) show that an adsorbed Ge atom (black) in strain-free Ge(111) pairs with a surface adatom (yellow) in the vicinity of a rest atom (red). The resulting *ad-dimer* sits on top of four surface dangling bonds (one from the rest atom plus three from backbond atoms) located at the vertices of a (111)-1 × 1 primitive cell. Two conspicuously stable geometries were found for the ad-dimer: (i) structures related to PES minima 1u (1f), where both atoms of the ad-dimer share a T_4 site [see Fig. 3(a)], and (ii) structures related to 2u (2f) minima, where the ad-dimer is displaced toward the rest atom, leaving the T_4 site occupied by a single atom [see Fig. 3(b)].

Regardless of the configuration adopted, each atom in the ad-dimer establishes three covalent bonds—one with its dimer partner, plus two with rest/backbond surface atoms—leaving two dangling bonds (one on each dimer atom). However, because of the different potential experienced by each atom, the resulting geometry is asymmetric.

The structure depicted in Fig. 3(b) is also representative of PES minima 3u (3f) and 4u (4f), related to the center adatoms (Fig. 2). However, according to Table I, the minima 3u (3f) and 4u (4f) are less stable than 2u (2f), probably because center adatoms are more strongly bonded to the substrate compared to corner adatoms, making them slightly more difficult to shift from their native T_4 site. This is consistent with the predicted exclusive formation of 1u (1f) ad-dimers involving corner adatoms, and it is in agreement with experimental STM results showing that Ge atoms on Si(111)-7 × 7 surface preferentially substitute Si corner adatoms in faulted HUCs [32].

According to Table I, sites 2u and 2f are the lowest energy sites in respectively unfaulted and faulted unstrained HUCs (for both 7 × 7 and 5 × 5 structures). We note that stable sites in the faulted HUC have slightly lower energy than the analogous sites in the unfaulted HUC. The preferential adsorption of adatoms on faulted Si(111)-7 × 7 HUCs at low coverage levels has been previously reported for a variety of atomic species [8,33–38]. Our results suggest that the

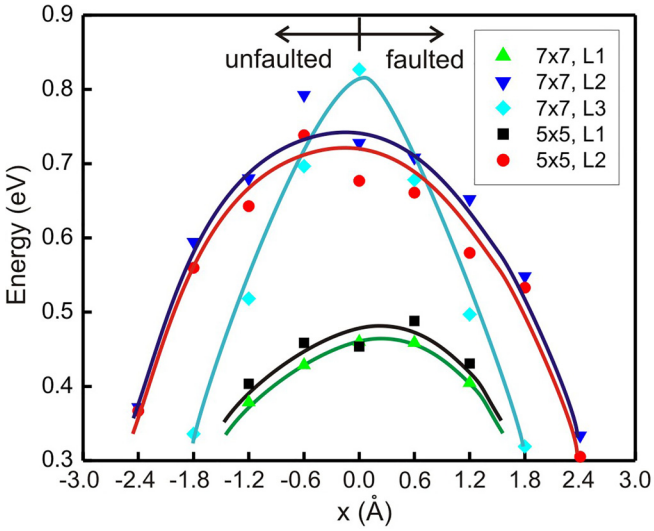

FIG. 4. Higher-energy section of PES profiles on unstrained Ge(111)-7 × 7 (L1–L3 paths) and Ge(111)-5 × 5 (L1, L2 paths) surfaces as indicated by dashed lines in Figs. 2 and 5(a), respectively. The energy of the most stable site (2f) is the origin of the energy scale for all profiles. Data points are from DFT calculations; solid lines are just guides to the eye.

same effect should be observed for Ge/Ge(111)-7 × 7 and Ge/Ge(111)-5 × 5 at low temperature.

Figure 2 clearly shows that PES minima are located around adatoms and rest atoms, forming a diffusion network within the HUCs with low energy barriers (about 0.2–0.3 eV). The reason for such low energy barriers rests on the distribution of dangling bonds within the HUCs, favoring a concurrent bond breaking and formation between the adsorbed atom and substrate atoms along the migration path.

Adjacent HUCs are separated by relatively high energy barriers (bright regions in Fig. 2). The reason for the high barriers is the absence of dangling bonds in regions along the dimer rows. Any border crossing performed by an adsorbed atom must break or substantially weaken its bonds to the substrate. According to the PES, the lowest energy barriers across the HUC border involve a hop of the adsorbed Ge atom over dimer atoms, either near the CH as indicated by the dashed line L1, or between dimers (as indicated by dashed lines L2, L3). Figure 4 shows the relevant section of three PES profiles across L1–L3 border crossings depicted in Fig. 2. For each profile in Fig. 4 the origin of the energy scale is the most stable site (2f) of the corresponding surface (either 7 × 7 or 5 × 5).

Clearly, the connection of sites 2u and 2f through L1 is the minimum energy path (MEP), with the saddle point located near the CH. The overall energy barrier for hopping from faulted to unfaulted HUCs along this path is about 0.4–0.5 eV (Fig. 4), and approximately 0.1 eV lower in the opposite direction (Table I). These barriers are distinctively lower than any other barrier for crossing the HUC border, and as explained below, they determine the long-range diffusivity of adsorbed Ge atoms across Ge(111)-7 × 7. The paths represented by lines L2 and L3 have considerably higher energy barrier (0.7–0.8 eV) and should have limited contribution to long-range surface diffusion. We note that the MEP on the 7 × 7 reconstructed surface depends on the chemical nature of the adsorbed atom, most notably on its valence and size. For example, the MEP for a Sr atom on Si(111)-7 × 7 crosses the HUC border right between surface dimers [8].

We suggest that the reason for the relatively low energy barriers is formation of a weak bond between the diffusing Ge adatom and dimer atom. Hybrid sp^3 states have several lobes responsible for the formation of strong σ bonds. These bonds determine the dimer structure and are all saturated within 7 × 7 and 5 × 5 structures. However, sp^3-hybrid states on atoms with bond angles departing from the perfect tetrahedral geometry develop wave function lobes with polarization opposite to the connected atoms [39]. Those lobes are prone to form weak covalent bonds, in the present case with the adsorbed Ge atom. We suggest that such bonds are crucial in the formation of the energy barriers, pretty much in the same way as they determine the small energy preference of T_4 over H_3 adsorption sites for many adsorbate species on Si(111) [40,41]. The higher barriers along the L2 and L3 paths as compared to L1 might be caused by a tight space (and stronger bonds) between dimers as compared to the space near the CH, so that formation of bonds with the adsorbed Ge atom is not so favorable. We also note that the adsorbed Ge atom does not form a bond with the atom in the middle of the CH; this atom is fully saturated [42].

The results presented above are in qualitative agreement with DFT data obtained for the Si/Si(111)-7 × 7 system [18]. The main difference is that the potential energy landscape for the case of Ge/Ge(111)-7 × 7 is flatter. For example, the MEP between HUCs in Si/Si(111)-7 × 7 also passes near the CHs and its energy barrier is approximately 1 eV. Additionally, energy barriers in the range 0.3–0.7 eV were found for the motion of adsorbed Si within the faulted and unfaulted HUC areas. Thus, while at $T = 300$ K a Si atom essentially roams within HUC areas, the crossing between them being hampered by a relatively high barrier, at $T = 400$ K hops between adjacent HUCs were experimentally observed [10]. However, according to our results, the effective hopping frequency (ν) between HUCs in Ge/Ge(111)-7 × 7 should be much higher than that in Si/Si(111)-7 × 7. Assuming that ν follows an Arrhenius dependence with T, we readily find that $\nu_{Ge}/\nu_{Si} \approx \exp[(E_{Si} - E_{Ge})/k_B T] \approx 10^8$ at $T = 300$ K, considering $E_{Si} = 1.0$ eV and $E_{Ge} = 0.5$ eV.

The authors of Ref. [18] have shown that migration via exchange with adatoms within the HUCs of Si/Si(111)-7 × 7 also involves a low energy barrier, and therefore should compete with atomic hopping inside HUC regions. An analogous mechanism may happen in Ge/Ge(111)-7 × 7 as well. However, the limiting step for long-range surface diffusion is HUC border crossing, and for that reason the exchange with adatoms was not examined. We also assume that HUC border crossings via exchange with dimer atoms is highly unlikely. This assumption is based on the fact that all dimer atoms within the 7 × 7 structure are fully saturated, and any atomic exchange must involve a costly bond breaking step.

Now we turn to the Ge/Ge(111)-5 × 5 system. Figure 5(a) shows the calculated PES for the adsorbed Ge atom on strain-free Ge(111)-5 × 5 surface. The image has clear similarities with the PES for Ge/Ge(111)-7 × 7 presented in Fig. 2.

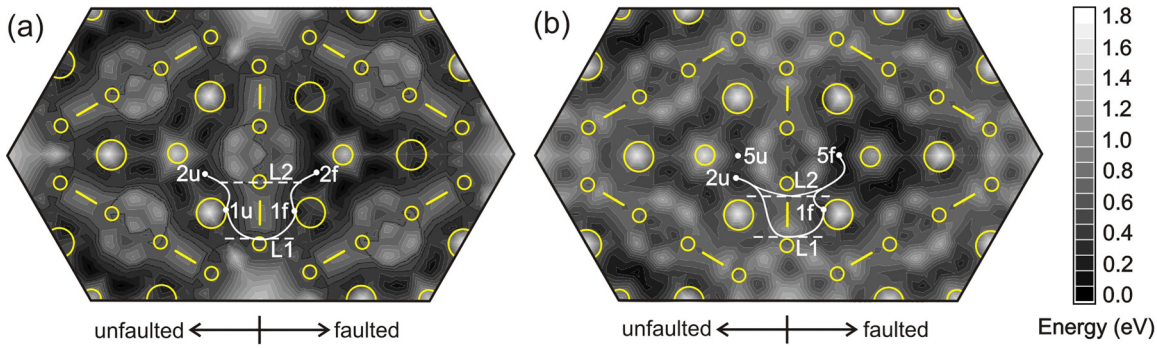

FIG. 5. PES for an adsorbed Ge atom on (a) unstrained and (b) 4% strain-compressed Ge(111)-5 × 5 surfaces. Dark (bright) regions indicate energy minima (maxima), and hence, favorable adsorption positions (unstable/transition-state regions). The contour spacing is 0.1 eV. Large circles are adatoms, medium circles are rest atoms, small circles with rods between them are dimers along HUC perimeter. White dots mark the deepest PES minima inside of unfaulted (u) and faulted (f) HUCs. Dashed lines across the HUC perimeter (L1, L2) mark the positions of calculated migration paths. Solid lines connecting the deepest energy minima [2u and 2f in (a) and 2u and 5f in (b)] in faulted and unfaulted HUCs are MEPs.

This is not surprising since both 5 × 5 and 7 × 7 consist of the same structural elements—dimers, adatoms, and stacking faults—arranged in the same fashion. The positions that correspond to adatoms at the faulted (unfaulted) HUCs are dark (bright) indicating that adatoms in the faulted part are easily shifted from their T_4 sites, thus forming ad-dimer configurations like the corner adatom sites of Ge(111)-7 × 7. Again, this is in agreement with experimental STM results [32].

Stable adsorption sites on 5 × 5 are located at 1u (1f) and 2u (2f) minima, with 2u (2f) having the lowest energy (as in the case of 7 × 7). The stable sites on 5 × 5 and 7 × 7 have identical local atomic arrangement [Figs. 3(a) and 3(b)]. The MEP between adjacent 5 × 5 HUCs [solid line in Fig. 5(a)] is also analogous to that in 7 × 7 HUCs: The crossing point is close to the CH (Fig. 2) along the L1 line. The resulting energy barrier along this MEP, represented by black squares, is very close to the one obtained for the Ge(111)-7 × 7 surface (Fig. 4). Clearly, the close structural similarity of 5 × 5 and 7 × 7 reconstructions leads to virtually the same energy barrier that limits long-range surface self-diffusion.

The diffusivity (D) describing the macroscopic surface diffusion of Ge atoms across many 5 × 5 or 7 × 7 cells is given by $D = D_0 \exp(-E_b/k_B T)$, where D_0 is a preexponential factor and E_b is an effective energy barrier. Elaborate kinetic Monte Carlo simulations could provide us with some figures for these quantities. Instead, we consider a simple surface diffusion model, which has the advantage of directly addressing the effects presented and questions raised in the Introduction.

The following analysis is based on two assumptions. The first is that (i) long-range diffusivity is mostly limited by the lowest HUC crossing barrier. Second, since the barriers for hoping within HUC areas are considerably lower than for HUC border crossing, we also assume that (ii) adsorbed atoms inside HUCs perform a fast random walk, which in the timescale between two consecutive border crossings allows them to span the whole HUC area and visit all stable sites with equal probability.

We start by comparing the surface diffusivity in 7 × 7 and 5 × 5 reconstructed surfaces. According to the above, hops between adjacent HUCs take place from sites near the CHs along L1 paths only (where the lowest energy barrier is located). The migrating atom can be described as effectively occupying the whole HUC area (S_{HUC}), and performing jumps between neighboring HUCs with length l equivalent to the HUC edge distance. The probability to find the adsorbed atom at corner sites ready for border crossing must be S_{cs}/S_{HUC}, where S_{cs} represents an effective surface area of all corner sites per HUC. Clearly, S_{cs} is the same for 7 × 7 and 5 × 5 structures, while their jump distance ratio is $l_{7\times7}/l_{5\times5} = 7/5$.

The surface diffusivity of an atom performing independent, randomly oriented jumps, across a two-dimensional lattice of stable sites, is generally given by [43]

$$D = gl^2\nu/4, \tag{1}$$

where in the present case $\nu = \nu_0 \exp(-E_b/k_B T)$ is the thermal frequency of jumps performed by the adsorbed atom between adjacent HUCs, g is the number of equivalent hoping routes available ($g = 3$ for hexagonal lattice), and ν_0 is the frequency of attempt for the jumps (across the HUC borders). Note that ν_0 is different than the attempt frequency for hops within the HUC. The latter quantity is often approximated to the Debye frequency of the material, ν_D, which to first approximation $\nu_0 \approx \nu_D(S_{cs}/S_{HUC})$ scales with l^{-2}.

Considering the above, and taking into account that E_b barriers for HUC border crossing are virtually the same in 7 × 7 and 5 × 5 reconstructed Ge(111) surfaces, it follows that the diffusivity is independent of l and therefore $D_{7\times7} = D_{5\times5}$. This explains why the effect of surface reconstruction was found negligible during diffusivity measurements [20].

Figure 5(b) shows the calculated PES for the adsorption of a Ge atom on a 4% strain-compressed Ge(111)-5 × 5 surface along lateral directions (corresponding to the lattice mismatch between Ge and Si lattice constants). From the above, we trust that the PES of the strained Ge(111)-7 × 7 surface should lead to similar results. One can see that the minima 1u and 2f are eliminated, while new minima—5u and 5f—emerge. The atomic structure relevant to 5u (5f) minima is shown in Fig. 3(c). According to this figure, the adsorbed Ge atom occupies the T_4 site between two neighboring adatoms. It connects to a rest atom (red) and two backbond atoms (green).

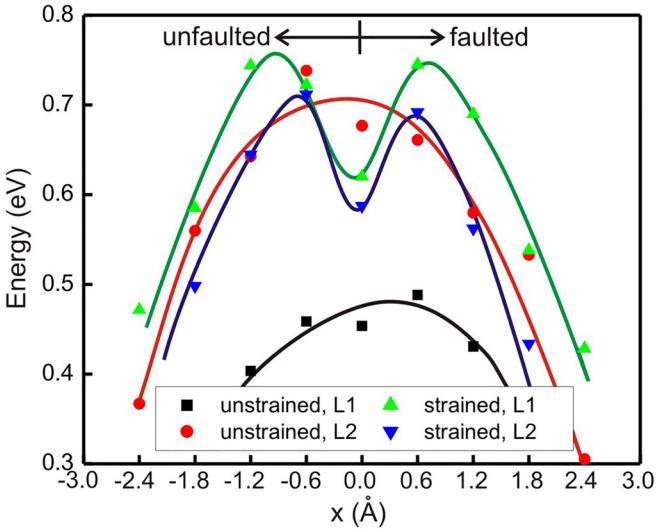

FIG. 6. Higher-energy section of PES profiles along L1 and L2 paths on (a) unstrained and (b) 4% strain-compressed Ge(111)-5 × 5 surfaces as indicated by dashed lines in Figs. 5(a) and 5(b), respectively. For each studied surface, the energy of the most stable site is considered the origin of the energy scale (2f for unstrained and 5f for compressively strained 5 × 5). Data points are from DFT calculations; solid lines are just guides to the eye.

The latter also connect to adatoms (yellow), and therefore are over-coordinated (have 5 neighbors).

It is interesting to note that while CHs on unstrained surfaces are clear energy maxima [Figs. 2 and 5(a)], several metastable sites are formed within these regions upon compression [Fig. 5(b)]. These sites are separated by large energy barriers, and they may trap adsorbed Ge atoms at low temperatures. Considering their locations, we suggest that they are caused by formation of backbonds with dimer atoms, which become closer under strain.

Figure 6 shows PES profiles along L1 and L2 lines crossing the HUC border on the strain-compressed Ge(111)-5 × 5 surface. For each profile in Fig. 6 the origin of the energy scale is the most stable site of the corresponding surface (2f and 5f for unstrained and strained 5 × 5, respectively). The profiles have the shape of a camel back, with a metastable midpoint located at the HUC edge, corresponding to the shallow minima observed near the CH in Fig. 5(b). Importantly, the energy barrier along the L1 line is significantly increased from 0.4–0.5 eV on unstrained 5 × 5 to 0.7–0.8 eV on strained 5 × 5. On the other hand, the change is not so conspicuous for the L2 profile. Both paths along L1 and L2 on strained 5 × 5 have similar energy barriers and both are likely to contribute to long-range surface self-diffusion [see solid lines in Fig. 5(b)]. The impact of the preexponential change to the diffusivity is expected to be minute (D should be enhanced by a factor of 2 if we account for twice the number of crossing points under strain). On the other hand, a change of E_b from 0.5 eV to 0.8 eV effectively hinders the adsorbed Ge atom within the HUC boundaries by decreasing D by a factor of 10^{-5} at $T = 300$ K.

Although the experimental data also suggest that the barrier increases with compression, the estimated change in the energy barrier (50–70 meV) [20,21] is less dramatic than the one anticipated theoretically. Much of the difference could be due to the fact that during the experiments the strain applied to the Ge(111)-7 × 7 surfaces was less than 4%. Indeed, previous calculations have shown that the 7 × 7 structure of the Ge(111) surface is stable in the ≈0%–1% compressive strain range [44]. Larger strain fields should convert the 7 × 7 into the 5 × 5 structure [44]. We suggest that the strain applied to the thin Ge(111)-7 × 7 layers reported in Refs. [20,21] was below 1%.

The increase of the energy barrier along the L1 line (near the CH) on the compressively strained surface can be caused by formation of stronger bonds at the 5f global PES minima [Fig. 5(b)], a destabilization effect at the saddle point, or both. To clarify this aspect, we compared the adsorption energy for (i) global PES minima sites and (ii) PES saddle points along L1 lines on unstrained and strained Ge(111) surfaces. We found that the adsorption energy on PES minima sites is almost identical for both surfaces. On the contrary, the adsorption energy on the L1 PES saddle point for the strained surface is lower than for the unstrained one by ≈0.27 eV. Therefore, the strain-induced enhancement of the barrier arises from destabilization of the PES saddle point.

The assumption on the nature of the weak bond between adsorbed Ge and dimer atoms made above can also explain the mechanism for bond weakening at the saddle point under compression. It is known that surface dimer bonds are stretched as compared to the bonds in the crystal bulk [our calculations give 2.617 Å for the length of Ge(111)-5 × 5 dimer bonds against 2.510 Å for bulk bonds], which is in agreement with our previous calculations [45]. When the surface is 4% compressed, the dimer bond lengths decrease toward the bulk value and become more stable (2.576 Å). A stronger σ bond means that more electron density is accumulated between dimer atoms and less density remains to share with a backbonded adsorbed Ge atom. The results obtained for Ge(111)-5 × 5 with the Ge atom adsorbed at the saddle point support our arguments: Accordingly, we find 2.516/2.494 Å dimer bond lengths and 2.513/2.606 Å bonds between the adsorbed Ge and dimer atom for the relaxed/compressed surface, respectively.

We finally note that the bonds connecting structure adatoms to surface backbond atoms in Ge(111)-5 × 5 become stronger under surface compressive strain. This is evident from the bright spots at the corresponding sites of faulted HUC in Fig. 5(b) as compared to dark spots at these sites in Fig. 5(a), suggesting that the structure adatoms become less prone to be displaced from their equilibrium positions.

IV. CONCLUSIONS

We investigated the effects of surface reconstruction (5 × 5 or 7 × 7) and strain on diffusion of adsorbed Ge atoms on Ge(111). The work was accomplished by accurately mapping the potential energy surface using first-principles calculations. According to the proposed model of surface diffusion, the adsorbed Ge atoms are very mobile within the half unit cell (HUC) areas, while long-range diffusivity is limited by a relatively larger barrier for crossing the rows of dimers (next to corner holes) which separate adjacent HUCs. We found that the change of surface reconstruction from 7 × 7 to 5 × 5

has negligible effect on long-range surface diffusion of Ge adsorbed atoms. This finding follows from identical energy barriers and atomistic mechanisms obtained for both 5×5 and 7×7 structures. We also found that surface compression strengthens the dimer bonds. Concurrently, that weakens the bond between dimer and adsorbed Ge atom at the saddle point, hence increasing the migration barrier of adsorbed Ge atoms across HUCs.

ACKNOWLEDGMENTS

R.A.Z. would like to thank the Novosibirsk State University for providing the computational resources. Cluster computations and paper writing were supported by the Russian Science Foundation (Project No. 19-72-30023). J.C. acknowledges the FCT through Projects No. UIDB/50025/2020-2023 and No. LA/0037/2020.

[1] H. Brune, K. Bromann, H. Röder, K. Kern, J. Jacobsen, P. Stoltze, K. Jacobsen, and J. Nørskov, Phys. Rev. B **52**, R14380(R) (1995).

[2] C. Ratsch, A. P. Seitsonen, and M. Scheffler, Phys. Rev. B **55**, 6750 (1997).

[3] Y.-W. Mo and M. G. Lagally, Surf. Sci. **248**, 313 (1991).

[4] Y.-W. Mo, J. Kleiner, M. B. Webb, and M. G. Lagally, Surf. Sci. **268**, 275 (1992).

[5] B. S. Swartzentruber, Phys. Rev. Lett. **76**, 459 (1996).

[6] D. J. Shu, F. Liu, and X. G. Gong, Phys. Rev. B **64**, 245410 (2001).

[7] E. Zoethout, O. Gürlü, H. J. W. Zandvliet, and B. Poelsema, Surf. Sci. **452**, 247 (2000).

[8] R. Zhachuk, B. Olshanetsky, J. Coutinho, and S. Pereira, Phys. Rev. B **81**, 165424 (2010).

[9] H. Uchida, T. Kuroda, F. B. Mohamad, J. Kim, K. Kashiwagi, K. Nishimura, and M. Inoue, Phys. Status Solidi B **241**, 1665 (2004).

[10] T. Sato, S. Kitamura, and M. Iwatsuki, Surf. Sci. **445**, 130 (2000).

[11] J. M. Gómez-Rodríguez, J. J. Sáenz, A. M. Baró, J.-Y. Veuillen, and R. C. Cinti, Phys. Rev. Lett. **76**, 799 (1996).

[12] L. Vitali, M. G. Ramsey, and F. P. Netzer, Phys. Rev. Lett. **83**, 316 (1999).

[13] H. Uchida, S. Watanabe, H. Kuramochi, J. Kim, K. Nishimura, M. Inoue, and M. Aono, Phys. Rev. B **66**, 161316(R) (2002).

[14] J. Mysliveček, P. Sobotík, I. Ošt'ádal, T. Jarolímek, and P. Šmilauer, Phys. Rev. B **63**, 045403 (2001).

[15] C. Polop, E. Vasco, J. A. Martín-Gago, and J. L. Sacedón, Phys. Rev. B **66**, 085324 (2002).

[16] H. Uchida, S. Watanabe, H. Kuramochi, M. Kishida, J. Kim, K. Nishimura, M. Inoue, and M. Aono, Surf. Sci. **532-535**, 737 (2003).

[17] O. Custance, I. Brihuega, J. M. Gómez-Rodríguez, and A. M. Baró, Surf. Sci. **482-485**, 1406 (2001).

[18] C. M. Chang and C. M. Wei, Phys. Rev. B **67**, 033309 (2003).

[19] K. Cho and E. Kaxiras, Surf. Sci. **396**, L261 (1998).

[20] V. Cherepanov and B. Voigtländer, Phys. Rev. B **69**, 125331 (2004).

[21] V. Cherepanov and B. Voigtländer, Appl. Phys. Lett. **81**, 4745 (2002).

[22] J. A. Venables, Surf. Sci. **299-300**, 798 (1994).

[23] K. Takayanagi, Y. Tanishiro, S. Takahashi, and M. Takahashi, Surf. Sci. **164**, 367 (1985).

[24] N. Troullier and J. L. Martins, Phys. Rev. B **43**, 1993 (1991).

[25] J. M. Soler, E. Artacho, J. D. Gale, A. García, J. Junquera, P. Ordejón, and D. Sánchez-Portal, J. Phys.: Condens. Matter **14**, 2745 (2002).

[26] A. García, N. Papior, A. Akhtar, E. Artacho, V. Blum, E. Bosoni, P. Brandimarte, M. Brandbyge, J. I. Cerdá, F. Corsetti, R. Cuadrado, V. Dikan, J. Ferrer, J. Gale, P. García-Fernández, V. M. García-Suárez, S. García, G. Huhs, S. Illera, R. Korytár *et al.*, J. Chem. Phys. **152**, 204108 (2020).

[27] J. P. Perdew, K. Burke, and M. Ernzerhof, Phys. Rev. Lett. **77**, 3865 (1996).

[28] H. J. Monkhorst and J. D. Pack, Phys. Rev. B **13**, 5188 (1976).

[29] T. Kawai and K. Watanabe, Surf. Sci. **357-358**, 830 (1996).

[30] K. Wang, G. Chen, C. Zhang, M. M. T. Loy, and X. Xiao, Phys. Rev. Lett. **101**, 266107 (2008).

[31] M. Krawiec and M. Jałochowski, Phys. Rev. B **87**, 075445 (2013).

[32] Y. L. Wang, H.-J. Gao, H. M. Guo, S. Wang, and S. T. Pantelides, Phys. Rev. Lett. **94**, 106101 (2005).

[33] S. Tosch and H. Neddermeyer, Phys. Rev. Lett. **61**, 349 (1988).

[34] E. Ganz, F. Xiong, I.-S. Hwang, and J. Golovchenko, Phys. Rev. B **43**, 7316 (1991).

[35] D. Tang, H. E. Elsayed-Ali, J. Wendelken, and J. Xu, Phys. Rev. B **52**, 1481 (1995).

[36] X. F. Lin, I. Chizhov, H. A. Mai, and R. F. Willis, Surf. Sci. **366**, 51 (1996).

[37] T. Hashizume, K. Motai, Y. Hasegawa, I. Sumita, H. Tanaka, S. Amano, S. Hyodo, and T. Sakurai, J. Vac. Sci. Technol. B **9**, 745 (1991).

[38] A. W. Akihiko Watanabe, M. Naitoh, and S. Nishigaki, Jpn. J. Appl. Phys. **37**, 3778 (1998).

[39] F. Bechstedt, *Principles of Surface Physics* (Springer-Verlag, Berlin, 2003).

[40] J. E. Northrup, Phys. Rev. Lett. **53**, 683 (1984).

[41] R. D. Meade and D. Vanderbilt, Phys. Rev. B **40**, 3905 (1989).

[42] A. A. Stekolnikov, J. Furthmüller, and F. Bechstedt, Phys. Rev. B **65**, 115318 (2002).

[43] L. T. Kong and L. J. Lewis, Phys. Rev. B **74**, 073412 (2006).

[44] R. Zhachuk, S. Teys, and J. Coutinho, J. Chem. Phys. **138**, 224702 (2013).

[45] A. E. Dolbak and R. A. Zhachuk, J. Exp. Theor. Phys. **133**, 44 (2021).